Effect of recycled powder and gear profile into the functionality of additive manufacturing polymer gears

Flaviana Calignano, Alessandro Bove, Vincenza Mercurio and Giovanni Marchiandi
Department of Management and Production Engineering (DIGEP), Politecnico di Torino, Turin, Italy

Abstract

Purpose – Polymer laser powder bed fusion (PBF-LB/P) is an additive manufacturing technology that is sustainable due to the possibility of recycling the powder multiple times and allowing the fabrication of gears without the aid of support structures and subsequent assembly. However, there are constraints in the process that negatively affect its adoption compared to other additive technologies such as material extrusion to produce gears. This study aims to demonstrate that it is possible to overcome the problems due to the physics of the process to produce accurate mechanism.

Design/methodology/approach – Technological aspects such as orientation, wheel-shaft thicknesses and degree of powder recycling were examined. Furthermore, the evolving tooth profile was considered as a design parameter to provide a manufacturability map of gear-based mechanisms.

Findings – Results show that there are some differences in the functioning of the gear depending on the type of powder used, 100% virgin or 50% virgin and 50% recycled for five cycles. The application of a groove on a gear produced with 100% virgin powder allows the mechanism to be easily unlocked regardless of the orientation and wheel-shaft thicknesses. The application of a specific evolutionary profile independent of the diameter of the reference circle on vertically oriented gears guarantees rotation continuity while preserving the functionality of the assembled mechanism.

Originality/value – In the literature, there are various studies on material aging and reuse in the PBF-LB/P process, mainly focused on the powder deterioration mechanism, powder fluidity, microstructure and mechanical properties of the parts and process parameters. This study, instead, was focused on the functioning of gears, which represent one of the applications in which this technology can have great success, by analyzing the two main effects that can compromise it: recycled powder and vertical orientation during construction.

Keywords 3D printing, Selective laser sintering, Laser powder bed fusion, Non-assembly mechanisms, Gear, Sustainable production

Paper type Research paper

1. Introduction

The design and construction of robots and other mechatronic projects, as well as automotive and aerospace engineering, have benefited in recent years from the continuous evolution of additive manufacturing (AM) technologies. Thanks to the layer-by-layer construction method, AM has a significant advantage to produce complex three-dimensional (3D) shapes, including gear wheel prototypes. These technologies allow the creation of directly multi-articulated mechanisms that integrate mechanical gears without further assembly operations. The benefits of non-assembly mechanisms are several: they reduce the time and the cost associated with the assembly operations, quickly evaluate the overall working space, check the limits of gear or joint and determine any interference between the parts (Chen and Lu, 2011). Some of the most extensively used AM processes to manufacture gears of various sizes and shapes are binder jetting, material extrusion (MEX), material jetting, vat photopolymerization and laser powder bed fusion (PBF-LB) (Budzik, 2011). Polymer gears have shown unique advantages over metal gears also in terms of sustainable production: low cost and weight, high efficiency, silent operation, operation without external lubrication, etc. The performance of AM gear has been investigated in recent years, especially for MEX technology (Buj-Corral and Zayas-Figueras, 2023). Zhang *et al.* (2020) investigated the manufacture of polymer gears using five different 3D printing nylon materials with the MEX process. Nylon 618 3D-printed gear provided the best wear performance among different filament materials. Nylon gears have also been investigated by Muminovic *et al.* (Muminovic *et al.*, 2022). In particular, the influence of the filling percentage on the types of failures and the service life of the gears was studied. Dimić *et al.* (2018) produced spur gears from

The current issue and full text archive of this journal is available on Emerald Insight at: **https://www.emerald.com/insight/1355-2546.htm**

Rapid Prototyping Journal
30/11 (2024) 16–31
Emerald Publishing Limited [ISSN 1355-2546]
[DOI 10.1108/RPJ-06-2023-0199]

The Authors greatly thank Dr Silvia Marola for analysis of powder. Vincenza Mercurio is funded by a PhD scholarship from the PON Research and Innovation 2014-2020 "Education and research for recovery – REACT-EU" according to the Ministerial Decree of August 10, 2021, No. 1061.

Received 17 June 2023
Revised 28 September 2023
Accepted 21 November 2023

polylactic acid (PLA) and acrylonitrile butadiene styrene (ABS) materials with the MEX process and performed wear tests at different speeds. The results showed that PLA material is stronger than ABS material. Harsha *et al.* (2021) tested PLA, ABS and nylon gears produced on MEX printers. In the comparison of polymeric gears, they stated that the nylon gear was the most durable one. Budzik (2011) analyzed the geometrical accuracy of gear wheels by pointing out that only when these sprocket models are oriented on the platform with the axis of rotation parallel to the construction axis can the accuracy of the teeth be increased. Tunalioglu and Agca (2022) investigated the wear resistance of polymeric spur gears produced by the MEX method. In this study, the wheels were produced with the axis parallel to the construction axis for reasons of accuracy.

Due to the absence of support structures, the polymer laser powder bed fusion (PBF-LB/P) process is one of the most promising AM technologies for building non-assembly mechanisms. This process is based on the interaction between a low-power laser (CO_2) and a thermoplastic powder bed. Figure 1 shows the phases of the process. As the laser melts the thermoplastic powder bed, the build platform moves downward, and a new powder layer is distributed by the recoating system. The powder layer is then preheated for a few tens of seconds by the thermal radiation from heater elements located on the top of the machine. The process is therefore repeated several times until the part is completed.

During the process, a low flow of nitrogen prevents the powder oxidation, and additional heating elements around the build chamber and the build platform are used to keep the whole environment close to the sintering point of the processed material. An important aspect of this process in terms of product sustainability is the possibility of recycling the powder used in a previous process. Figure 2 shows the powder recycling process in more detail. The regenerated powder is generally obtained by mixing 50% of new powder, and it is representative of the feedstocks used in industrial settings. In the PBF-LB/P process, only 10–20% of the powder in the part bed chamber is used to create the parts (Bourell *et al.*, 2014; Dotchev and Yusoff, 2009; Mielicki *et al.*, 2012). The rest of the powder is used to support the parts during processing. These undergo physical and chemical deterioration in the manufacturing processes, including preheating, sintering and cooling (Dadbakhsh *et al.*, 2017a; Feng *et al.*, 2019), but can be recycled and reused for further applications. Deteriorated powders have reduced surface morphologies, larger and more complex molecular chains, reduced fluidity and deteriorated thermal and mechanical properties, which make direct reuse difficult (Chen *et al.*, 2018; Dadbakhsh *et al.*, 2017a; Dotchev and Yusoff, 2009). Furthermore, the low utilization rate of the powder and the cost of the powder (around 150 €/kg) induce powder reuse (Feng *et al.*, 2019; Wudy and Drummer, 2019; Yang *et al.*, 2023). Therefore, recycling and reuse are necessary for a sustainable PBF-LB/P process.

In recent years, relevant works have been published on the physical and mechanical characteristics of parts produced using regenerated PA12 powders. Yang *et al.* (2020) proposed a process control method to maximize the reusability of aged and extremely aged PA12 powders. Based on intercalated heating, pretreatment and mixing of powder materials, they can print samples with mechanical properties even higher than the

Figure 1 Phases of SLS process

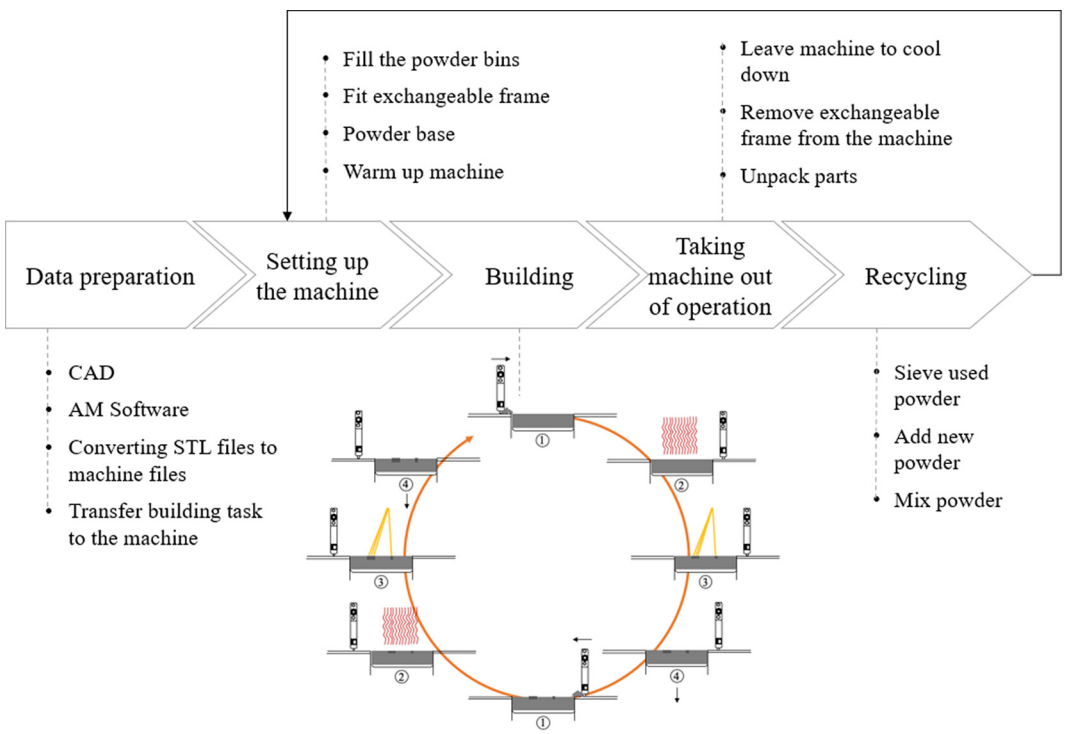

Source: Figures are by the authors

Figure 2 Powder recycling phases

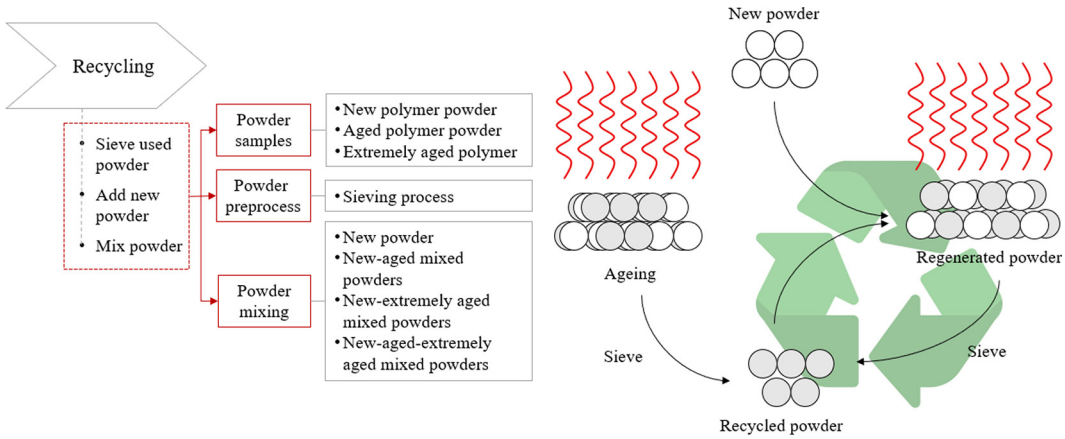

Source: Figures are by the authors

current values used in the industrial sector: samples with 18.04% higher tensile strength and 55.29% larger elongation at break using as much as 30% of extremely aged powders compared to the reference sample. Calignano *et al.* (2021) compared PA12 parts printed by PBF-LB/P and HP multi-jet fusion (MJF). The results showed that the material properties can also vary as a function of the rotation of the piece with respect to the construction direction. MJF technology offers higher breaking strength, while PBF-LB/P trumps other calculated characteristics. Depending on sample orientation and printing technology, porosity levels and pores have different morphology and distribution in the sample. Feng *et al.* (2019) transformed recycled PA12 powders from the PBF-LB/P process into filaments for use with the MEX process. Yao *et al.* studied the effects of powder recycling on the tensile properties of PA12 samples printed in different build orientations, as well as on the resulting microstructural characteristics and the crystalline structures of the powders. The results show that there are few differences in shape, size and powder distribution between virgin and recycled powders, but more fractured, small and smooth sphere powders are distributed in adhered powders.

The possibility therefore of reusing the powders several times, of being able to use the entire building volume through an operation called nesting, and the absence of support structures that reduce waste materials and post-processing times for their removal make this appealing technology for industries to reduce the number of parts and integrate gear systems. The ability to create components with already-assembled mechanical parts can significantly reduce production times as well as costs. Furthermore, for example, toys for children, such as toy cars and carillons, with mechanisms made in one piece can be much safer as they do not contain small parts that can be disassembled.

However, as highlighted above, only a few studies have focused on the use of this process to produce gear wheels. Gears with nonstandard geometries have been studied by Andrei *et al.* (2005). The gears were manufactured with their axis perpendicular to the construction direction. The authors highlight the relatively poor accuracy of the tooth flank due to the low accuracy of the file and the relatively low accuracy of the PBF-LB/P process. Pandian *et al.* (2022a) compare the flexural fatigue performance of spur gears manufactured with two types of Nylon through PBF-LB/P (using Nylon 12) and traditional plastic injection molding (IM) process (using Nylon 66). The results showed that PBF-LB/P gears have a longer flexural fatigue life in the high-cycle fatigue region than IM gears. In contrast, this effect was not important in the low-cycle fatigue region. The reason for the performance lies in the fatigue strength of the PBF-LB/P gears, which varies due to the different thermal behaviours in the two fatigue cycle regimes. The layered structure of the gear helped prevent crack propagation in the PBF-LB/P process. The same authors (Pandian *et al.*, 2022b) have shown that the orientation angle affects the bending fatigue strength. The PBF-LB/P gears manufactured in an on-edge configuration exhibited lower fatigue life than IM gears. The nylon-based gears were made using three different manufacturing techniques, namely, IM, PBF-LB/P and machining, by Jain and Patil (2022). The study highlighted the high roughness of the PBF-LB/P process, which affects the accuracy of the tooth profile.

The purpose of this study was to identify the main problems relating to the precision of the wheels produced using the PBF-LB/P process to be able to exploit the advantages deriving from the use of this technology and highlighted previously (high recycling of the powder and absence of supports). To evaluate the effect on the functionality of the mechanical gear integrated into a component, the clearance between the parts, the gear surface and the sintered mass around the gear surface using recycled powder were considered. Since the thermal change along the z-axis (build direction) is typical of the process, replicas of the reference gears are produced in two different locations in the build chamber.

2. Materials and methods

The main process problems encountered in the PBF-LB/P gear literature (Figure 3) are:

- shaft-wheel orientation with axis perpendicular to the construction direction (subsequently called "vertical") results in lower accuracy than components produced with axis parallel to the construction axis (called "horizontal"); and
- staircase effect and process parameters that negatively affect the tooth profile.

Figure 3 Schematic representation of the main factors affecting the accuracy of the parts produced in PBF-LB/P

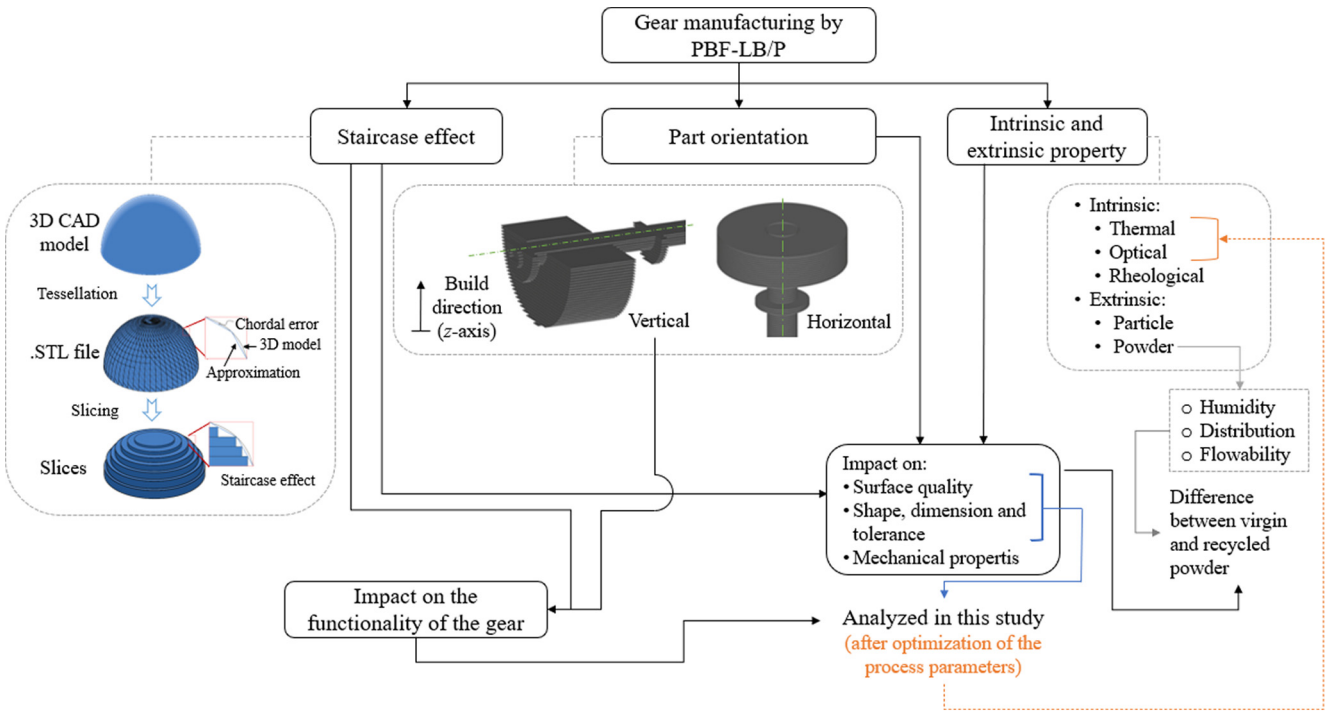

Source: Figures are by the authors

The layering mechanism of the additive processes, the powder size and shape distribution, the orientation of the part, the laser settings (laser power, scan speed, etc.), the aging stage of the powder, as well as the machine processing settings, are just some of the causes that have been identified in the literature as having the greatest impact on PBF-LB/P surfaces (Pilipovic *et al.*, 2016; Vetterli *et al.*, 2017). Various studies in the literature have focused on analyzing the effects of intrinsic (thermal, optical and rheological) and extrinsic (particles and powder) properties (Schmid and Wegener, 2016) on the accuracy of the components produced with this technology (Petzold *et al.*, 2019). The combination of these properties can lead, if not well optimized, to the formation of streaks and a nonhomogeneous powder deposition, which lead to a low density of the sintered part and reduced mechanical properties. More critical is the deformation effect of the sintered layers during processing due to thermal variations during construction progress and/or during cooling. This phenomenon leads to reduced geometric accuracy and can even lead to process interruption when out-of-plane deformation leads to collision between the part and the recoating blade.

Therefore, starting from these considerations, the study focused on some aspects that affect the geometric accuracy, which in turn makes the functionality of a gear ineffective: the recycled powder and the orientation. This study was divided into three phases:

1 optimization of parameters to avoid dimensional variations and deformations induced by thermal gradients;
2 analyze the relationship between optimized parameters and recycled powder (industrial standard) on a standard type of gear positioned at two different levels in the chamber and in two orientations; and
3 maintain the functionality of the gears if it is necessary to produce them with the axis of the wheels parallel to the direction of construction (the worst condition).

2.1 Samples

When designing gears using PBF-LB/P technology, it is necessary to consider the effects due to the hot environment and high temperatures that can lead to the impossibility of removing the powder within the clearance between the shaft and wheel. Therefore, starting from the literature (Allison *et al.*, 2017; Chen and Lu, 2011; Kruf *et al.*, 2006; Mavroidis *et al.*, 2001; Minetola *et al.*, 2020), a clearance (c) of 0.55 mm has been fixed. Table 1 and Figure 3 show the design parameters and the integrated mechanical gear, respectively. The integrated mechanical gear is designed as a conventional hub shaft coupling (Figure 4). It consists of two parts: a shaft and a wheel. The wheel is positioned between two collars obtained on the shaft to prevent the wheel from sliding off the shaft during the locking test. The two collars are sufficiently spaced to allow access to the wheel-shaft connection area from both sides of the wheel and to facilitate the removal of non-melted powder trapped inside the clearance, manually or possibly by shot-blasting. The gear design [Figure 4(a)] is described by the configuration of two different wheels having as fixed values the root circle diameter (d_f), the reference circle diameter (d), the addendum diameter (d_a), the number of teeth and the inner diameter (d_i) and by two variable parameters, namely, the shaft diameter (d_s) and the wheel thickness (t_w) (Table 1). The variation of d_s and t_w allows for investigating the effect of the presence of thermal masses that accumulate heat by

Table 1 Design parameters

Fixed parameters					
Root circle diameter d_f [mm]	Reference circle diameter d [mm]	Addendum diameter d_a [mm]	No. of teeth	Module m (teeth) [mm]	Inner diameter d_i [mm]
30.5	33	35	33	1	4
Variables parameters					
Shaft diameter d_s [mm]					10, 14
Wheel thickness, t_w [mm]					8, 10, 14
Distance internal diameter groove d_g [mm]					2.5, 3
Grove width k [mm]					5.55, 7.55
Grove depth t [mm]					12.10, 16.10

Building orientation: horizontal			Building orientation: vertical		
Sample	d_s [mm]	t_w [mm]	Sample	d_s [mm]	t_w [mm]
A1	10	8	*C1*	10	8
A2	10	10	*C2*	10	10
A3	10	14	*C3*	10	14
B1	14	8	*D1*	14	8
B2	14	10	*D2*	14	10
B3	14	14	*D3*	14	14

Source: Tables are by the authors

Figure 4 (a) Integrated mechanical gear; (b) first geometric modification with slots; (c) second geometric modification with a groove between wheel and shaft

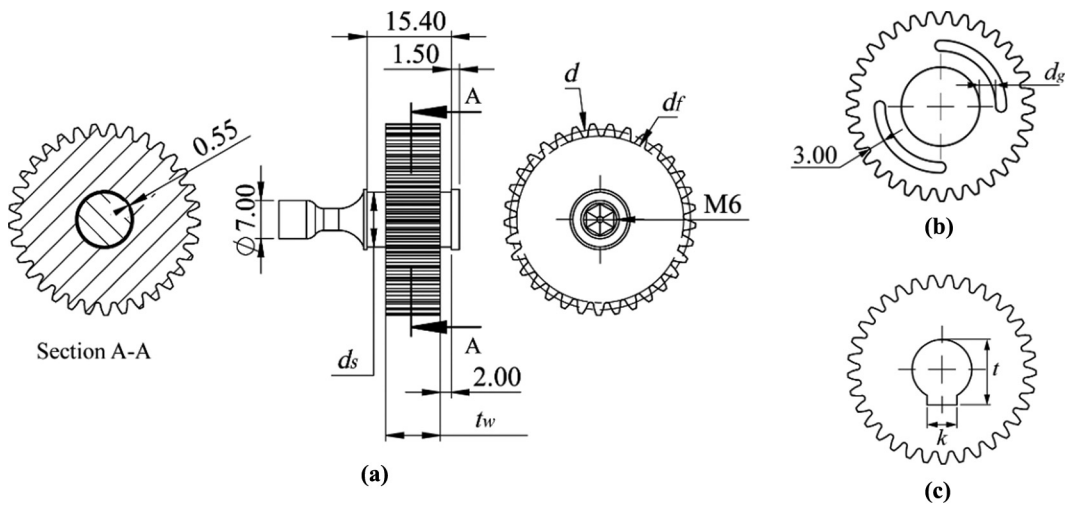

Source: Figures are by the authors

closing the gap and providing certain inertia to temperature fluctuations. The presence of these masses may also contribute to a greater sintering effect and therefore compromise the rotation of the wheel concerning the shaft. For this reason, two other configurations were designed and analyzed. The wheels have been modified by inserting:

1 two slots to reduce the mass around the area between the wheel and the shaft. Three values have been chosen for the distance (d_g) between the internal diameter and the slots, considering maintaining a certain strength. The distance between the slots and the d_f has been set at 3 mm [Figure 4(b)]; and
2 a groove between the shaft and the wheel as in the case of transmission wheels [Figure 4(c)]. The groove has been deliberately designed to be rectangular to reduce the stair-case effect typical of the process. The wheels were oriented with the groove at 0, 90, 180 and 270 degrees, both with the wheel axis parallel to the construction axis and with the perpendicular axis.

Each sample has been marked with a bas-relief number on the top of the collar at the end of the shaft. At the opposite shaft end, a hexagonal hole has been designed to accommodate an M6 Allen key to force the shaft rotation to the wheel and unlock the mechanism after the cleaning process. To unlock the joint samples, a torque wrench was used with a torque equal to 4 N/m for all specimens. The torque is applied to remove the obstruction due to the residual powder inside the clearance or, in the worst case, to break the micro fusion points in the wheel-shaft interface due to the sintering.

X-ray CT scanning (GE Phoenix v|tome|x s) was performed to nondestructively examine the gear. The process parameters

used for the scans were a voltage of 100 kV, a current of 50 μA and a voxel size of 50.224 μm. GOM Inspect software was used to compare CAD model and CT scanning 3D model. A stereo microscope, LEICA S9i, equipped with an integrated 10 MP camera, was used to analyze the different evolving profiles tested on the gears.

2.2 Process

The samples were produced using an EOS FORMIGA P110 Velocis machine. The machine has a theoretical construction volume of 200 mm × 250 mm × 330 mm. However, a portion of this build volume equal to 40 mm × 30 mm × 330 mm is occupied by the thermocouple that measures the temperature of the powder bed for each layer and therefore is excluded by the working volume.

During the cooling, the part undergoes a volume contraction, which is due to the difference in the density of polymers between the melt state and the cooled, rigid state. High cooling rates may cause fast volume contraction, part distortions and dimensional errors. The distortion is mainly referred to as curling and warping effects (Mazzoli, 2013; Raghunath and Pandey, 2007; Shi *et al.*, 2004; Soe *et al.*, 2013) that may occur during the building and cooling phases. During the building phase, due to excessively rapid cooling of the individual layers in the process chamber, variations may occur, especially at the outer edges, of the quantity of powder deposited. Instead, during the cooling phase, failure to observe the cooling time after the end of the job and therefore too rapid removal of the container containing the component made or premature opening of the door of the removal chamber will result in rapid cooling of the overall job. This induces cooling of the uneven part from the bottom up and from the outside to the inside, which can cause the part to distort in the lower layers (Figure 5).

The shrinking behavior varies according to the processed material and may be different along the axis. During the process, the thermal gradients are partly compensated by the heating systems and the preheating phase and prevent shrinkage. However, during the cooling phase, owing to the conduction effects, the high cooling rate throughout the walls of the build chamber (called exchangeable build frame in Figure 5) and low conductivity of the polymeric powder cause a thermal gradient in the *xy*-plane and along the build direction (z-axis), with warmer central areas [Figure 5(b)]. In general, cooling rates are slow because of the reliance on conduction through the powder bed and the low thermal conductivity of polymer powders (Yuan *et al.*, 2011). To compensate for the part shrinkage [Figure 5(c)] during the cooling phase, the printed part is larger than the final desired dimensions. To consider the volume shrinkage during the cooling phase, uniform scale factors were used for *x*- and *y*-axes equal to 3.35% and 3.27%, respectively, while along the build direction (*z*-axis), the scale factor was varied linearly from 2.6% (z = 0 mm) to 2% (z = 300 mm). In addition to shrinkage, the beam offset is another parameter that influences the accuracy of parts produced by PBF-LB/P. Beam offset includes laser spot diameter, heat-affected area and deflection angle during laser scanning (Wang, 1999). The beam offset value was fixed to 0.29 mm. The beam diameter d is 0.42 mm (Figure 6). However, the diameter of the area where the particles are sintered is slightly larger than that physical diameter of the beam (effective sintering diameter d_e), i.e. about 0.5 mm. The process parameters used for the hatching are laser power of 21 W, scan speed of 2,500 mm/s and hatching distance of

Figure 5 (a) Schematic representation of the EOS Formiga P110 Velocis (front view); (b) shrinkage behavior in building volume; (c) shrinkage (defined as a change in size) and warpage (defined as a change in shape)

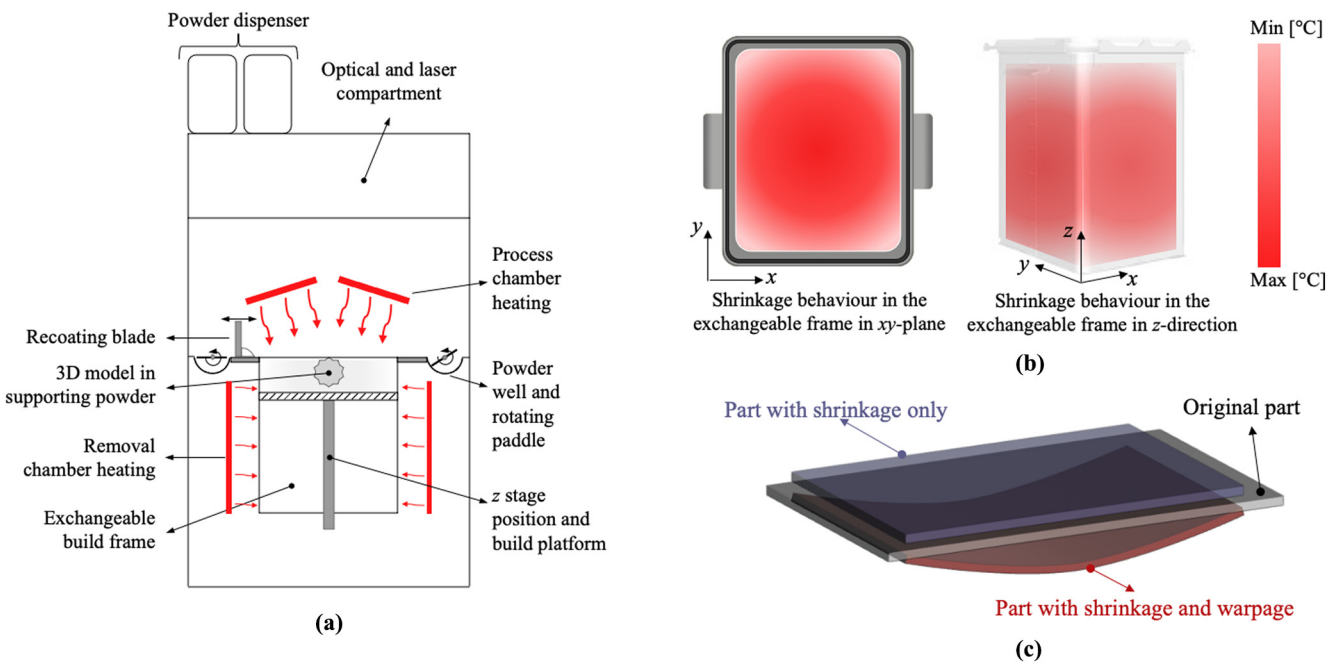

Source: Figures are by the authors

Figure 6 Schematic representation of the main parameters of the PBF-LB/P process

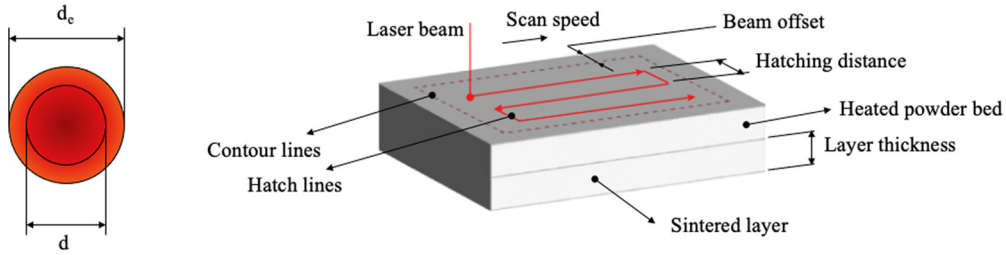

Notes: de = effective beam diameter; d = physical beam diameter
Source: Figures are by the authors

0.25 mm. Hatching distance (also called hatch spacing or scan spacing) is the separation between two consecutive laser beams (Figure 6). It is measured by a distance from the center of one beam to the center of the next beam. The layer thickness was set equal to 0.10 mm, and the waiting time between the end of a layer and the subsequent powder deposition was set equal to 5 s. This time avoids a strong thermal gradient that may be generated between the warm, melted layer and the fresh powder, which is at the environmental temperature. The process chamber and removal chamber temperatures were set to 169°C and 154°C, respectively. After the production, the total cooling time was 4 h. After that, the samples were cleaned manually with a brush from loose powder, and then the powder into the clearance has been gently removed by shot peening with glass beads and subsequently with compressed air. Thanks to this set and the process parameters used, the minimum feature size that can be obtained is 0.25 ± 0.02 mm.

The placement and orientation of the part in the build chamber are elements to be taken into consideration because, again due to heat, they can affect the quality of the part (Goodridge *et al.*, 2012). The samples have been replicated at different heights of the build chamber, i.e. 5 mm and 160 mm away from the build platform. The samples were equally spaced along the *x*- and *y*-axes to avoid heat accumulation areas.

2.3 Material

The samples were fabricated using regenerated PA2200 (trade name of EOS GmbH for PA12) powder, a mixture of new and reused powder, and mixed with a rotating system, keeping the relative humidity above 30%. Figure 7 shows the virgin powder and the reused powder.

The powders have an irregular shape with the presence of small satellites on the surface of the powders. It is possible to see some smaller particles of lighter color in both powders. A feature of the PA2200 material is the incorporation of titanium dioxide (TiO_2) to improve its whiteness, flowability and absorption properties (Schmid, 2018; Verbelen *et al.*, 2016). It also acts as a nucleating agent (Olejarczyk *et al.*, 2020). Figure 7c shows the differential scanning calorimetry (DSC) thermogram for the powder used in this study. The heating and cooling cycles are very similar, and the melting *T* reproduces the manufacturer's claims well. The sintering window is about 12°C for the new powder and increases to 16°C for the processed ones. The heat associated with melting also shows no significant changes after PBF-LB/P, indicating no significant degradation. In cooling, the behavior is perfectly reproducible.

After the first use with 100% new powder, about 10% of the new powder is sintered, and about 90% of the unsintered powder becomes aged powder during the PBF-LB/P process. The aged powders were exposed to typically 2–10 cycles (Dadbakhsh *et al.*, 2017a). After 10% of the aged powder is used, approximately 40% is removed as a waste powder (mainly from regions around the part due to excessive heating contact of part surfaces) from the remaining 90% of the aged powder. The remaining 50% aged powder is mixed with 50% virgin powder, called mixed powder. The experimental tests were therefore carried out considering the data from the literature (Dadbakhsh *et al.*, 2017a; Yang *et al.*, 2020) and from the manufacturer on the maximum number of cycles that the aged powder should do to keep the characteristics unaltered, i.e. eight cycles.

3. Results and discussion

3.1 Recycled powder effect

The results are shown in Table 2. As it is possible to see, in addition to the two cases, locked or unlocked, there is a third case, unlocked in the axial direction but locked in the rotational one. Analyzing Table 2, some differences are found between 100% virgin powder (named below "case 1") and 50% virgin powder and 50% recycled powder for five cycles (named below "case 2"). The thickness of the wheel and its orientation (vertical or horizontal axis with respect to the direction of construction) affect the rotation or otherwise of the gear for a wheel diameter equal to 10 mm. If the thickness of the wheel is below 10 mm, the wheel rotates around the shaft in both cases. In case 2, if the thickness is greater than 10 mm, if the wheel is built horizontally, only the presence of a 3 mm slot allows it to rotate; otherwise, the gear is blocked. If the wheels are built vertically, they can be unlocked along the axial direction, but there is no possibility to rotate the wheel around the shaft. In the case of the wheel with a shaft diameter of 14 mm, there is different behavior between the wheel geometries and the construction orientation for the 8 mm and 10 mm thicknesses. While the wheels with a thickness of 14 mm (shaft diameter of 14 mm) have the same behavior regardless of the orientation. The wheels are unlocked only if built vertically with a thickness of 8 mm and the presence of a slot of 2.5 mm or a grove. In case 1, the wheels with grove are unlocked, unlike in case 2.

Figure 7 SEM images of powder particles

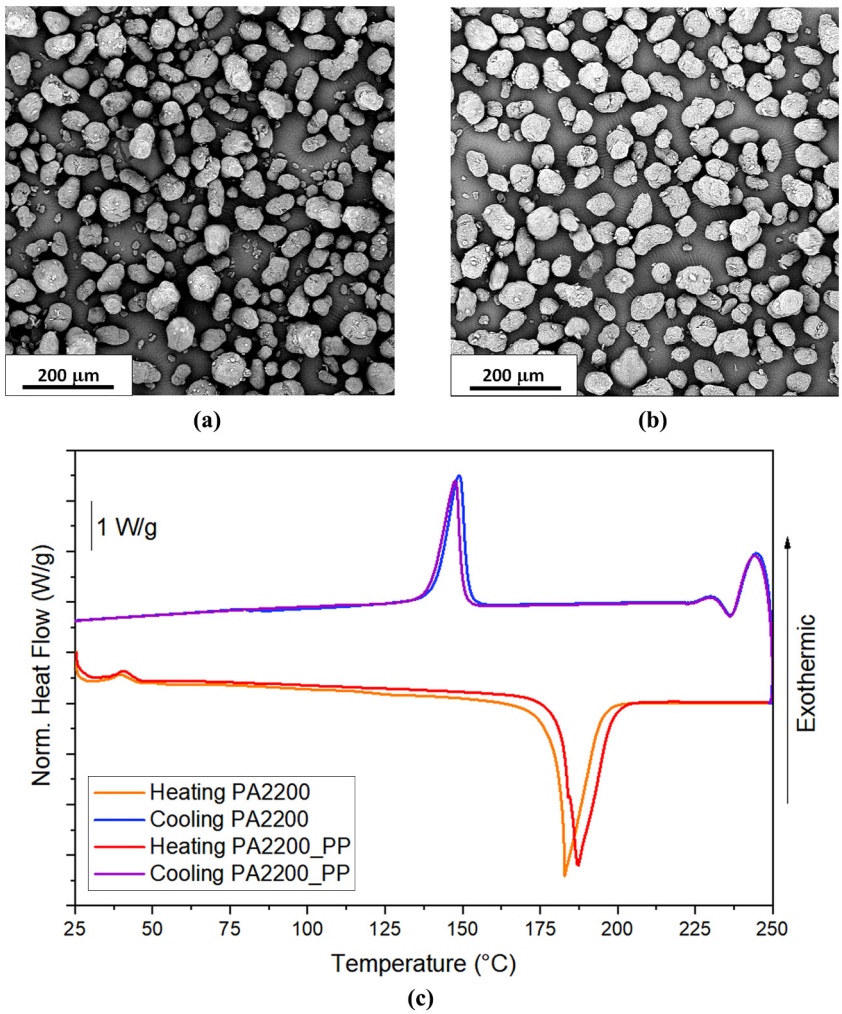

Notes: (a) Virgin; (b) recycled powder; (c) DSC plot of the virgin and recycled powder
Source: Figures are by the authors

Figure 8 depicts the X-ray CT scanning images of the deformation of the wheels according to the orientation during construction. Contrary to what happens in case 1 [Figure 8(c)], in case 2 there is a greater deviation from the ideal plan for the last layers (purple line in Figure 8). This could be attributed to an increase in molecular weight originating from a possible cross-linking of the polymeric material leading to an increase in melt viscosity, which can also occur as the powder ages (Kobayashi and Yang, 2023; Kuehnlein *et al.*, 2010; Wudy and Drummer, 2019). Considering wheels *A2*, there is a different behavior in case 2 between wheels *A2_s1* and *A2_s2* [Figure 8(a)] in the gap area (red line in Figure 8).

Curling is the result of shrinkage and warping generally associated with deformation (curved rather than flat profile) of a downward-facing surface of a part due to thermal stresses and layerwise shrinkage stresses. Observing the enlargement of the *A2_s1* in Figure 8(a), it is possible to notice that the curling does not start from the initial layers in which instead a warping effect is seen more. As known in the literature (Senthilkumaran *et al.*, 2009), there is a greater variation in shrinkage than the nominal size of a sample in the *y*-direction due to the inhomogeneous nature of the shrinkage. This inhomogeneity is influenced by two factors: thermal gradients and coating movements. The thermal gradient during the building and cooling process differs with the different lengths of the strips in the sample as well as with the aging of the powder. The reason for this lies in the variation of the energy density. It is defined as the ratio of laser power to the product of scan speed times hatching distance and layer thickness. A hatching with scanning vector [Figure 9(c)] of greater length has a longer delay time (calculated as the ratio between the distance traveled by the laser beam to scan two consecutive points and the scan speed) between consecutive exposures of the same point, while a shorter length has a shorter delay time (Jain *et al.*, 2009). Added to this is the effect of solidification variation due to aged powder; the powder bed at the point of construction of the part

Table 2 Locked and unlocked integrated mechanical gears

Horizontal						Vertical					
Sample	**Unlocked**		**Locked**		**Axial unlocked**	**Sample**	**Unlocked**		**Locked**		**Axial unlocked**
A1	Δ	x				*C1*	Δ	x			
A2			Δ	x		*C2*			Δ		x
A3			Δ	x		*C3*			Δ		x
B1			Δ	x		*D1*			x		
B2			Δ	x		*D2*			x		
B3			Δ	x		*D3*			x		
Slot 1 (d_g = 2.5 mm)											
A1_s1	Δ	x				*C1_s1*	Δ	x			
A2_s1			Δ	x		*C2_s1*			Δ		x
A3_s1			Δ	x		*C3_s1*			Δ		x
B1_s1			Δ		x	*D1_s1*		x	Δ		
B2_s1			Δ	x		*D2_s1*			Δ		x
B3_s1			Δ	x		*D3_s1*			Δ	x	
Slot 2 (d_g = 3 mm)											
A1_s2	Δ	x				*C1_s2*	Δ	x			
A2_s2	x		Δ			*C2_s2*		x	Δ		
A3_s2			Δ	x		*C3_s2*			Δ		x
B1_s2			Δ	x		*D1_s2*		x	Δ		
B2_s2			Δ	x		*D2_s2*			Δ	x	
B3_s2			Δ	x		*D3_s2*			Δ	x	
Grove 1 (k = 5.55 mm, t =12.10 mm)											
A1_g	Δ	x				*C1_g*	Δ	x			
A2_g	Δ		x			*C2_g*		Δ			x
A3_g	Δ		x			*C3_g*		Δ			x
Grove 2 (k = 7.55 mm, t =16.10 mm)											
B1_g	Δ		x			*D1_g*	Δ	x			
B2_g	Δ		x			*D2_g*		Δ			x
B3_g	Δ		x			*D3_g*		Δ	x		

Notes: Legend: Δ for 100% virgin powder; x for 50% virgin and 50% recycled powder (five cycles)
Source: Tables are by the authors

retains heat for a relatively long period. Also, shrinkage in longer length zones is very different from that in shorter length zones, as shrinkage in large geometries tends to be retarded due to internal stresses (Singh *et al.*, 2012). Therefore, the difference in thickness of 0.5 mm between the two wheels in the areas of the slots leads to a different solidification and cooling time, which affects the geometric accuracy differently. Considering the second factor, when the recoater blade spreads the powder, it exerts a theoretically uniform pressure, but it is not uniform due to the encounter with the sintered areas, which will have a different behavior. The movement of the recoater is along the *x*-direction of the machine. The amount of powder and therefore its weight vary in position along the *y*-direction as it settles during movement from one side of the build platform to the other. The powder will be greater at the starting point of the application and less at the end point after application. During sintering, the zone will tend by gravity, due to its weight, to be lower than the powder plane, and therefore, even if the platform lowers by a given layer, the height of the layer will be different in the various zones of the bed. Therefore, the pressure exerted on the new layer will be different because in the next layer, the blade goes in the opposite direction to the previous layer, and therefore there is no uniformity in the *y*-direction. This nonuniform shrinkage can be reduced via scaling factors; however, the size of the area that is sintered based on the geometry of the component has a high influence due to thermal shrinkage and may therefore not be compensated for by scaling factors. Furthermore, it must be considered that the theoretical height of the layer of powder increases in the first layers due to the difference in volume between the powder and the solidified material [Figure 9(b)]. The more the molecular weight increases, the more this difference increases, leading to micrometric mountains of powder in the empty areas of the wheel that create sintering areas in the gap.

In the wheels built vertically, in addition to the typical staircase effect, there is a greater roundness in the area between the wheel and the shaft due to the powder that remains partially sintered. This means that although they can free themselves by creating an axial movement, they are unable to impart a rotation. By applying such a force as to break the weak links between the unsintered particles and overcome the friction force generated between the faces of the gear and the unsintered powder, also due to the surface roughness, it is possible to unlock the system by imparting an axial movement of the wheel on the shaft. However, due to deformation in some

Figure 8 (a), (b) and (d) Deformation of samples with recycled powder according to orientation; (c) sample built with 100% virgin powder

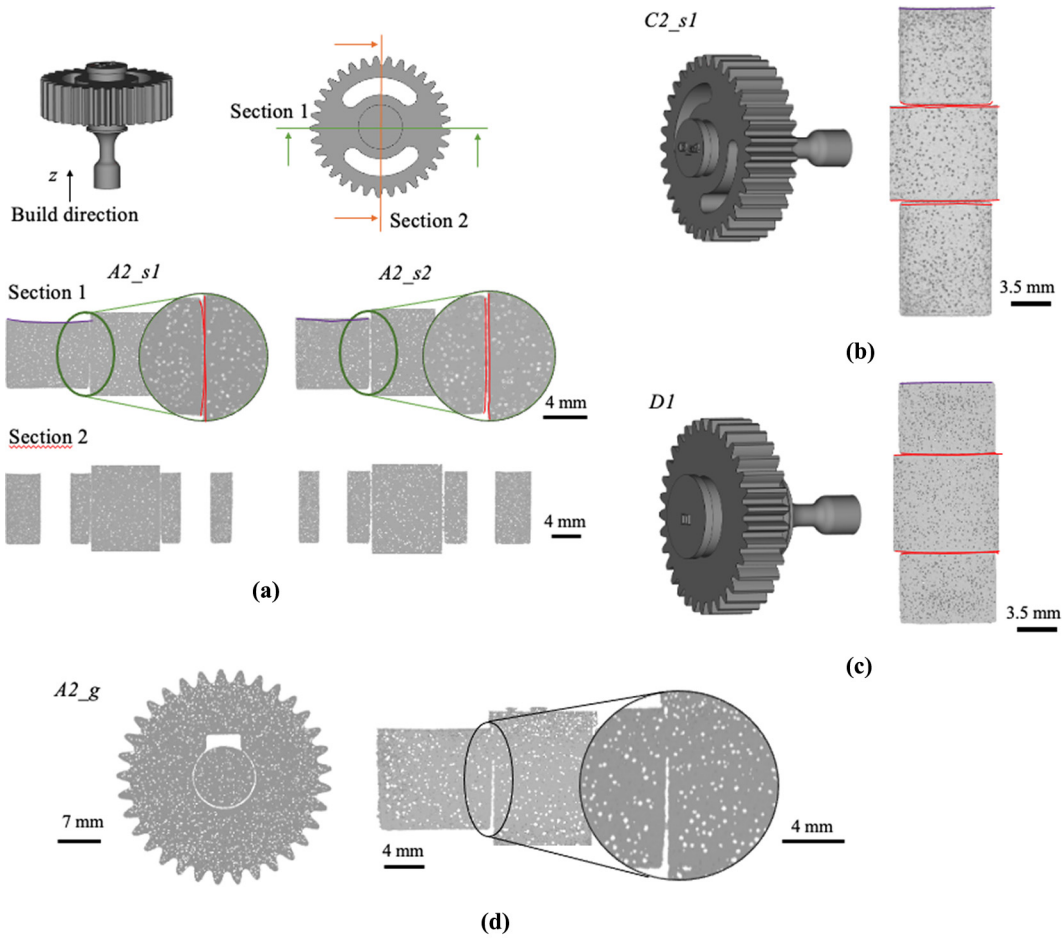

Source: Figures are by the authors

areas depending on the staircase effect (Figure 10), it is not possible to impart a rotational movement to the wheel with respect to the shaft. From the CT scan image [Figure 10(b)], it is possible to see how the staircase effect becomes accentuated compared to the model simulated in the software [Figure 10(a)]. When a grove is created, the effect is reduced, allowing rotation for wheel thickness less than 10 mm. The thickness of the wheel of 10 mm, therefore, becomes a limit condition in this case.

In case 1, the wheels with the groove are released thanks to the reduction of mass in the area between the shaft and the wheel and the reduced surface roughness compared to case 2, which allows reducing the formation of small, sintered areas in the areas with higher peaks of roughness. With virgin powder and with powder mixed below five cycles, proper sintering occurs with enough sintered material and good viscosity that allows necks to form between adjacent particles, resulting in a dense structure with low porosity and better accuracy dimensional.

If the powder is recycled beyond five cycles, especially eight cycles, there is a high deterioration of the gear geometry (Figure 11). Figure 11 shows the high lack of accuracy compared to the CAD model. The number of teeth has been reduced to allow for better analysis of their accuracy. The deviation in some areas, especially at the level of the teeth, can be up to 2 mm compared to the CAD model. The color variations on the surface of the wheel (Figure 11) are due to what is called "orange peel." As highlighted in the literature (Chen *et al.*, 2018), the aged powder presents an increase, albeit slight, in the peak melting temperature and at the same time a decreasing trend in the melting enthalpy of the powder. The reduced melting enthalpy can cause more severe secondary sintering of the surrounding powders, and thus affect the surface precision of the PBF-LB/P part, such as "orange peel" texture (Dotchev and Yusoff, 2009). Therefore, as powder recycling increases, the dimensional precision of the part is reduced compared to the original part, and the definition of the shape in the contours, and therefore of the profile of the teeth, is difficult to obtain. The change in the surface quality of the parts can also be attributed to the change in the size and shape distribution of the powder particles with the increase in the number of reuse cycles. The exposure of the powders to the high processing temperature during the process inevitably causes a thermal degradation, which affects the flowability by decreasing it and thus leading to reduced coalescence and consolidation during construction (Dadbakhsh *et al.*, 2017b; Shackleford *et al.*, 2021). This phenomenon worsens as the number of reuse cycles increases, leading to reduced surface quality of printed parts.

Figure 9 (a) Build process; (b) difference between leveling height and powder layer height; (c) schematic representation: hatching, line of the vector and different temperature based on the length of the vector

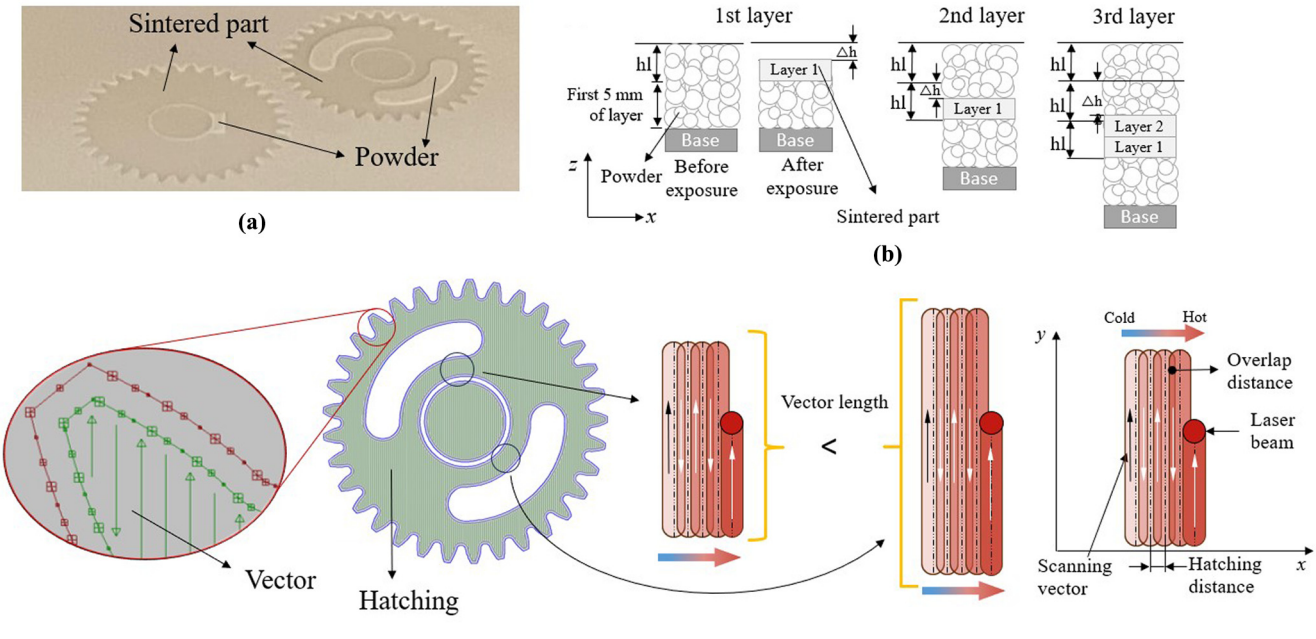

Source: Figures are by the authors

Figure 10 (a) Stl model with overlapping slices and (b) CT scan image

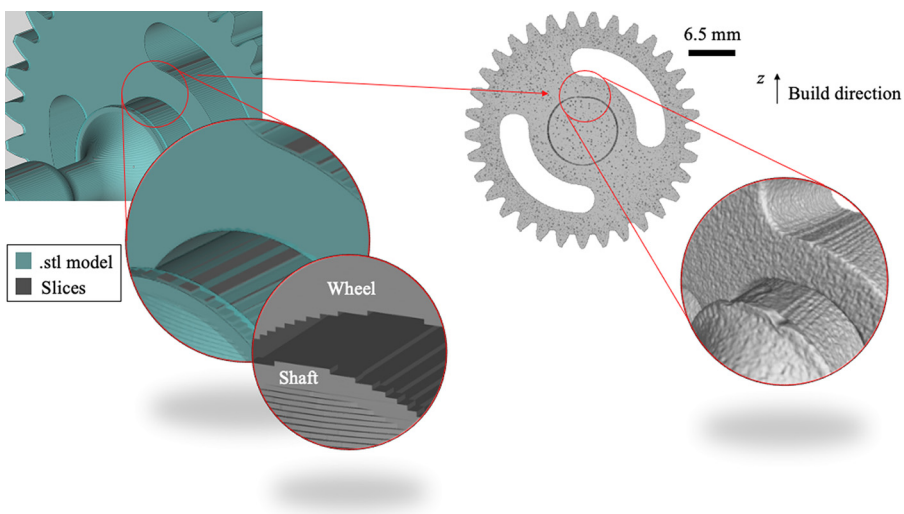

Source: Figures are by the authors

3.2 Gear profile

An analysis of the wheel teeth revealed a problem that can be detected in the process itself. If the wheel is built with the axis perpendicular to the construction direction, the slicing will affect the geometry of the tooth (Figure 12).

The profile of some teeth is modified during the creation of the sections, which have a height equal to the layer thickness, in this case, 0.10 mm. This change causes the wheels, when coupled, to lock at a certain point in their rotation. This does not happen if the wheels are built with their axis parallel to the direction of construction. Ghanekar *et al.* (Watson, 2003) have shown that by decreasing the thickness of the layer it is possible to obtain a decrease in the surface roughness and the staircase effect. However, in an industrial manufacturing environment, reducing

Figure 11 Comparison of CAD model and CT scanner 3D model. Gear is produced with 50% virgin and 50% recycled powder after eight cycles

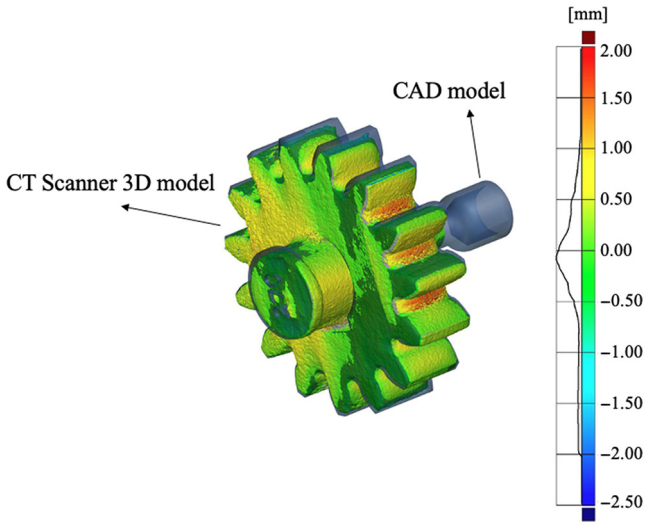

Source: Figures are by the authors

the layer thickness of parts would not be sustainable in the long term as it implies longer construction times and therefore an increase in costs associated with them (electricity, etc.). Therefore, to try to find a possible solution to the problem that is also suitable for the industrial sector, a further study on the evolving profile of the tooth (according to BS ISO 21771:2007 standard) has been performed. Theoretically, the evolving profile of a single gear depends on the reference circle diameter *d*. For this reason, different evolving profiles have been tested on gears with different diameters. The vertical building orientation of the gears can significantly alter the tooth profile for staircase effects or deformations; therefore, extra complications are included to compare the behavior of the gears under the worst possible conditions. The design parameters of the conducted study are reported in Table 3. The parametric equations (Spiegel and Seymour Lipschutz, 2009) allow the generation of the tooth's evolving profile in a bi-dimensional space, as reported in Figure 13. Gears with different diameters and tooth profiles have been produced in both build orientations. Specific support has been designed and produced to evaluate the continuity of rotation coupling of the gears produced with different profiles and diameters.

To test the functionality of the manufactured gears, a gearbox has been designed, produced and assembled. The apparatus used is schematized in Figure 14 (the record of the performed test is reported in Supplementary_material_appendix_1). The purpose of this test is to verify the correct motion of the gearbox with no interruptions and the correct transmission of the torque between the motor and the user. Also, the performances in terms of mechanical resistance can be highlighted by applying a resistant torque in output and verifying the correct motion of the gearbox.

Table 3 Design parameters for the study of the teeth profile

Gear	d [mm]	Evolving radius [mm]
1	15	7.5
2	30	7.5
3	45	7.5
4	15	15.0
5	30	15.0
6	45	15.0
7	15	22.5
8	30	22.5
9	45	22.5

Source: Tables are by the authors

Figure 12 Effect of slicing on CAD geometry

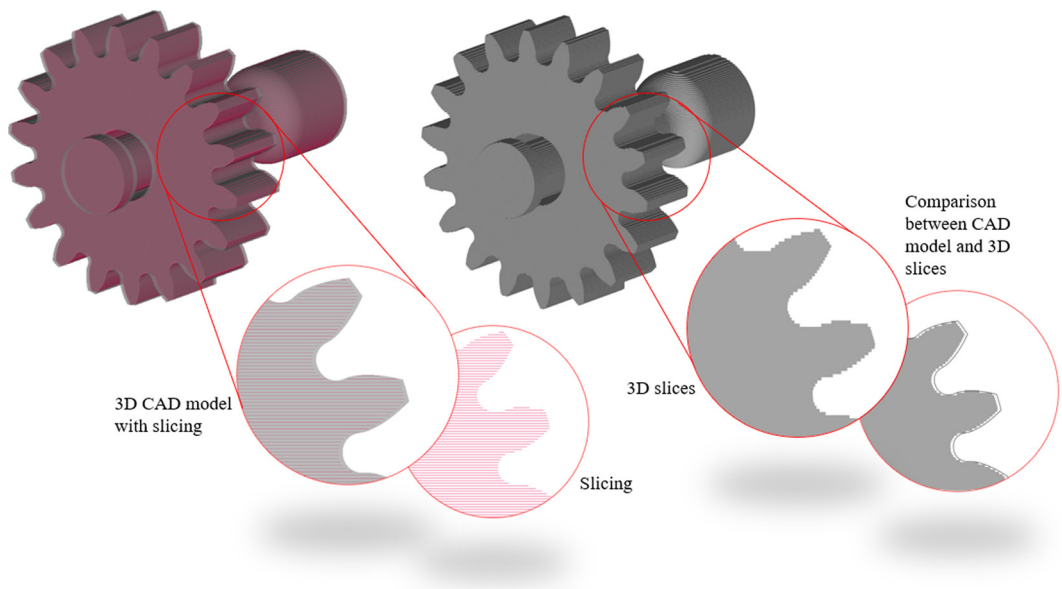

Source: Figures are by the authors

Figure 13 Different tooth profiles produced and their generative parametric equations

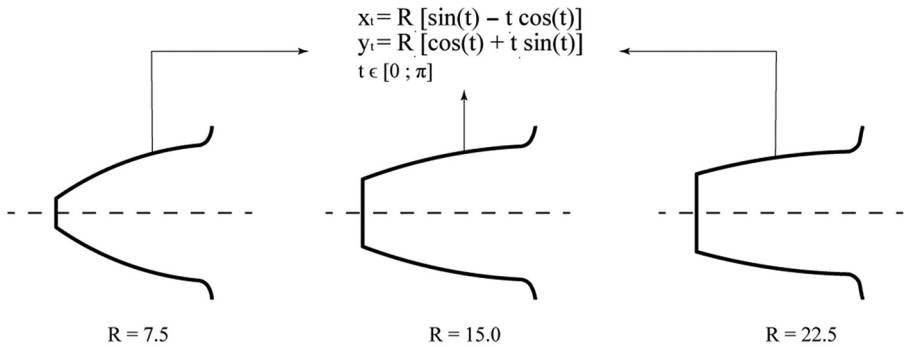

Source: Figures are by the authors

Figure 14 Test apparatus used for the functionality tests on the produced gears

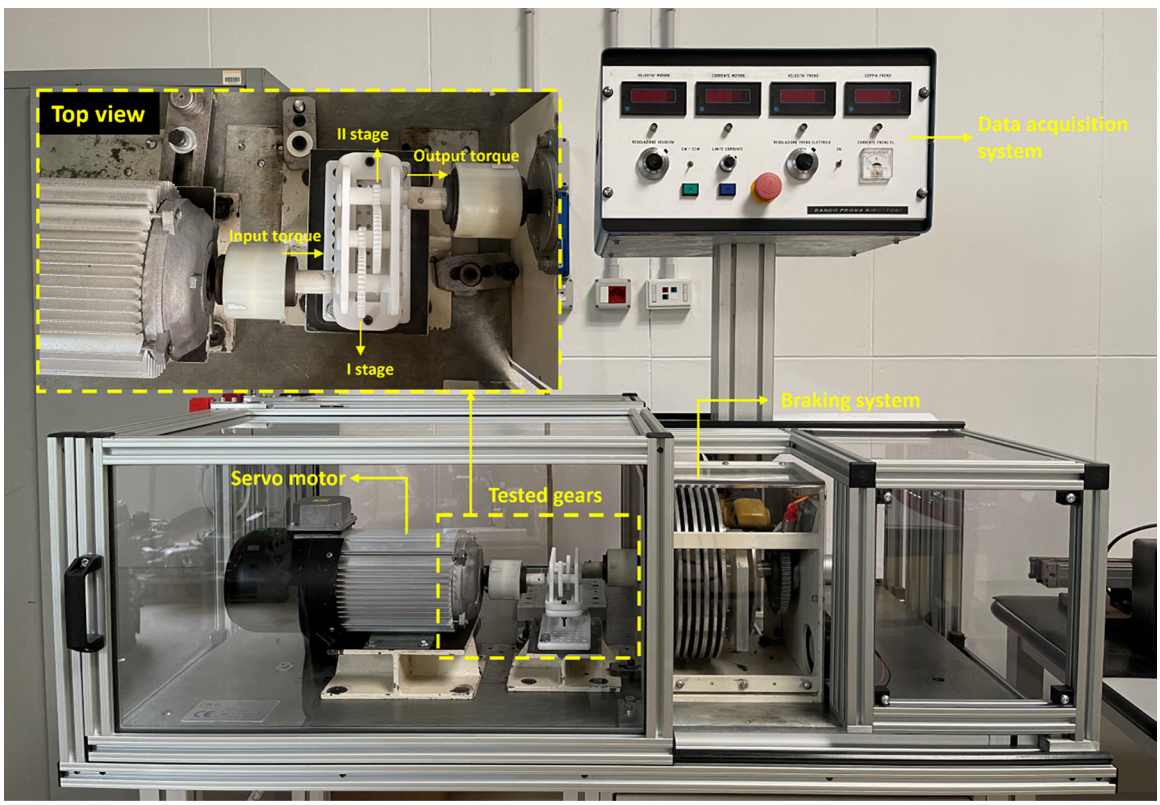

Source: Figures are by the authors

The greasing test performed revealed that the tooth profile has an influence on the discontinuity in rotation only for vertical gears. The different profiles used on the gears oriented horizontally result in uniform contact between the teeth during the meshing test, and a continuous rotation is guaranteed for all diameters and evolving radii. The gears vertically oriented showed, in some cases, discontinuity in the contact and rotation for specific coupling of profiles. In general, imperfection due to the building orientation and the degree of recycling of powder, which is highlighted in Figure 15, can trigger the generation of other defects on the head of the teeth, affecting the continuity in rotation. More specifically, for all diameters tested, the evolving radius of 15 mm showed good behavior during the greasing test. The coupling between gears 2 and 7 revealed the worst behavior in terms of continuity in rotation.

The modification of the tooth profile brought about by flaws in the recycle grade, the incorrect design or the building orientation are all factors affecting the functionality of the gears and their suitability for use in particular working conditions,

Figure 15 Stereomicroscope image of the different evolving profiles tested on the gears produced in the vertical orientation with fully recycled powder

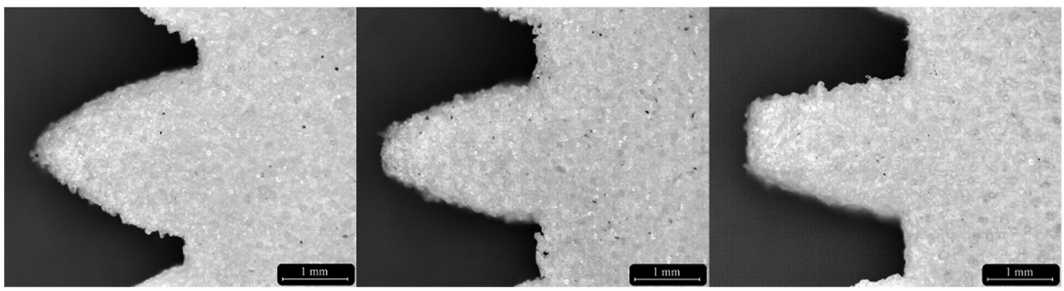

(a) **(b)** **(c)**

Notes: (a) Gear 2; (b) gear 5; (c) gear 8
Source: Figures are by the authors

which is one of the test's most significant findings. In comparison to horizontally oriented gears, maintaining the proper tooth profile in relation to the gear diameter is generally more crucial for vertically oriented gears. The results for mechanical resistance and torque gearbox have been confirmed by coupling the gears with, respectively, 15 mm and 45 mm of diameter in the benchmarks tested. As depicted in Figure 14, the addition of two distinct velocity stages enables the output torque to be amplified and a successful outcome for the gears' applicability. With constant transmitting efficiency, 360 rpm input speed and 1.6 Nm breaking torque have been achieved with vertically oriented gears. A maximum input speed of 720 rpm with no breaking torque applied has been reached. Operational dysfunction may be caused by the interaction of the staircase effect, the amount of powder recycling and the improper tooth profile relative to the gear's diameter. The staircase effect cannot be regarded as a factor in the development of tooth profile defects on horizontally oriented gears, and the gears' functionality can be easily respected. The staircase effect becomes more significant when affecting the reliability of recycled powder parts for vertically oriented gears.

4. Conclusion

The study focused on the analysis of a kinematic mechanism to understand the effect of recycled powder on accuracy, starting from a well-established fact in the literature, i.e. the gap required to have a kinematic mechanism already assembled during the process. By applying a value known in the literature, such as 0.55 mm of gap, it has been shown that the geometry of the kinematic mechanism and the reused powder can make this value unsuitable. This suggests that kinematic design requires knowledge of the state of the powder. The variation in the size and shape distribution of the powders at different reuse stages would lead to variations in the roughness and density of the powder bed packing, and the resulting surface corrugations would lead to variations in the dimensions of the parts. As reported in the literature, the surface quality and dimensional accuracy of the sintered parts decreased with increased number of powder reuse cycles. Furthermore, it was found that when the powder is recycled five times with the addition of 50% new powder, the parts produced have a rough surface finish, a phenomenon referred to as orange peel.

The presence of the staircase effect has led some researchers to consider only one orientation, the horizontal one, as suitable for the construction of gears. The building orientation of the mechanisms is not always controllable in complex assemblies. The results highlight the need to maintain the correct tooth profile in relation to the gear diameter, especially for vertically oriented gears. However, both orientations can highlight problems: in the case of gears oriented horizontally (wheel axis parallel to the construction axis), the main problems will concern deformations and the reduction of clearances due to thermal effects; in the case of vertically oriented gears (wheel axis perpendicular to the construction direction), the problems are mainly due to the scaling effect and an incorrect choice of the tooth profile with respect to the gear diameter. In both cases, the more the powder is recycled, the more it can compromise the precision and, therefore, the functionality of the gear.

References

Allison, J., Sharpe, C. and Seepersad, C.C. (2017), "A test part for evaluating the accuracy and resolution of a polymer powder bed fusion process", *Journal of Mechanical Design*, Vol. 139 No. 10, doi: 10.1115/1.4037303.

Andrei, L., Epureanu, A., Andrei, G., Birsan, I. and Walton, D. (2005), "Synthesis and analysis of plastic curved-face-width spur gears", VDI Berichte.

Bourell, D.L., Watt, T.J., Leigh, D.K. and Fulcher, B. (2014), "Performance limitations in polymer laser sintering", *Physics Procedia*, Vol. 56, p. 157, doi: 10.1016/j.phpro.2014.08.157.

Budzik, G. (2011), "The use of the rapid prototyping method for the manufacture and examination of gear wheels", *Advanced Applications of Rapid Prototyping Technology in Modern Engineering*, pp. 339-364, doi: 10.5772/22848.

Buj-Corral, I. and Zayas-Figueras, E.E. (2023), "Comparative study about dimensional accuracy and form errors of FFF printed spur gears using PLA and nylon", *Polymer Testing*, Vol. 117, p. 107862, doi: 10.1016/j.polymertesting.2022.107862.

Calignano, F., Giuffrida, F. and Galati, M. (2021), "Effect of the build orientation on the mechanical performance of polymeric parts produced by multi jet fusion and selective

laser sintering", *Journal of Manufacturing Processes*, Vol. 65, doi: 10.1016/j.jmapro.2021.03.018.

Chen, Y. and Lu, J. (2011), "Minimise joint clearance in rapid fabrication of non-assembly mechanisms", *International Journal of Computer Integrated Manufacturing*, Vol. 24 No. 8, pp. 726-734, doi: 10.1080/0951192X.2011.592995.

Chen, P., Tang, M., Zhu, W., Yang, L., Wen, S., Yan, C., Ji, Z., Nan, H. and Shi, Y. (2018), "Systematical mechanism of polyamide-12 aging and its micro-structural evolution during laser sintering", *Polymer Testing*, Vol. 67, doi: 10.1016/j.polymertesting.2018.03.035.

Dadbakhsh, S., Verbelen, L., Verkinderen, O., Strobbe, D., Van Puyvelde, P. and Kruth, J.P. (2017a), "Effect of PA12 powder reuse on coalescence behaviour and microstructure of SLS parts", *European Polymer Journal, Elsevier*, Vol. 92 No. May, pp. 250-262, doi: 10.1016/j.eurpolymj.2017.05.014.

Dadbakhsh, S., Verbelen, L., Verkinderen, O., Strobbe, D., Van Puyvelde, P. and Kruth, J.P. (2017b), "Effect of PA12 powder reuse on coalescence behaviour and microstructure of SLS parts", *European Polymer Journal*, Vol. 92, doi: 10.1016/j.eurpolymj.2017.05.014.

Dimić, A., Mišković, Ž., Mitrović, R., Ristivojević, M., Stamenić, Z., Danko, J., Bucha, J. and Milesich, T. (2018), "The influence of material on the operational characteristics of spur gears manufactured by the 3D printing technology", *Strojnicky Casopis*, Vol. 68 No. 3, pp. 261-270, doi: 10.2478/scjme-2018-0039.

Dotchev, K. and Yusoff, W. (2009), "Recycling of polyamide 12 based powders in the laser sintering process", *Rapid Prototyping Journal*, Vol. 15 No. 3, pp. 192-203, doi: 10.1108/13552540910960299.

Feng, L., Wang, Y. and Wei, Q. (2019), "PA12 powder recycled from SLS for FDM", *Polymers*, Vol. 11 No. 4, doi: 10.3390/polym11040727.

Goodridge, R.D., Tuck, C.J. and Hague, R.J.M. (2012), "Laser sintering of polyamides and other polymers", *Progress in Materials Science*, Vol. 57 No. 2, doi: 10.1016/j.pmatsci.2011.04.001.

Harsha, K.M., Seetharama Rao, Y. and Jagannadha Rao, D. (2021), "Comparison of wear behaviour of polymer spur gears using FDM process", *IOP Conference Series: Materials Science and Engineering*, Vol. 1168 No. 1, doi: 10.1088/1757-899x/1168/1/012028.

Jain, M. and Patil, S. (2022), "Comparative analysis of surface characteristics of nylon based polymer gears manufactured by different techniques", *Materials Today: Proceedings*, Vol. 63, doi: 10.1016/j.matpr.2022.02.050.

Jain, P.K., Pandey, P.M. and Rao, P.V.M. (2009), "Effect of delay time on part strength in selective laser sintering", *The International Journal of Advanced Manufacturing Technology*, Vol. 43 Nos 1/2, doi: 10.1007/s00170-008-1682-3.

Kobayashi, R. and Yang, M. (2023), "Nondestructive observation of the surrounding powder in the vicinity of polymer laser-sintered specimens for understanding orange peel formation", *Rapid Prototyping Journal*, Vol. 29 No. 7, doi: 10.1108/RPJ-08-2022-0268.

Kruf, W., van de Vorst, B., Maalderink, H. and Kamperman, N. (2006), "Design for rapid manufacturing functional SLS parts", *Intelligent Production Machines and Systems – 2nd I*PROMS Virtual International Conference*, 3-14 July 2006, doi: 10.1016/B978-008045157-2/50070-5.

Kuehnlein, F., Drummer, D., Rietzel, D. and Seefried, A. (2010), "Degradation behavior and material properties of PA12-plastic powders processed by powder based additive manufacturing technologies", *Annals of DAAAM and Proceedings of the International DAAAM Symposium*.

Mavroidis, C., DeLaurentis, K.J., Won, J. and Alam, M. (2001), "Fabrication of non-assembly mechanisms and robotic systems using rapid prototyping", *Journal of Mechanical Design*, Vol. 123 No. 4, pp. 516-524, doi: 10.1115/1.1415034.

Mazzoli, A. (2013), "Selective laser sintering in biomedical engineering", *Medical & Biological Engineering & Computing*, Vol. 51 No. 3, doi: 10.1007/s11517-012-1001-x.

Mielicki, M., Wegner, A., Gronhoff, B., Wortberg, J. and Witt, G. (2012), "Prediction of PA12 melt viscosity in laser sintering by a time and temperature dependent rheological model", *RTejournal*, Vol. 32, pp. 1-32.

Minetola, P., Calignano, F. and Galati, M. (2020), "Comparing geometric tolerance capabilities of additive manufacturing systems for polymers", *Additive Manufacturing*, Vol. 32, p. 101103, doi: 10.1016/j.addma.2020.101103.

Muminovic, A.J., Pervan, N., Delic, M., Muratovic, E., Mesic, E. and Braut, S. (2022), "Failure analysis of nylon gears made by additive manufacturing", *Engineering Failure Analysis*, Vol. 137, doi: 10.1016/j.engfailanal.2022.106272.

Olejarczyk, M., Gruber, P. and Ziólkowski, G. (2020), "Capabilities and limitations of using desktop 3-D printers in the laser sintering process", *Applied Sciences*, Vol. 10 No. 18, doi: 10.3390/APP10186184.

Pandian, A.K., Gautam, S.S. and Senthilvelan, S. (2022a), "Comparison of the bending fatigue performances of selective laser sintered and injection moulded nylon spur gears", *Proceedings of the Institution of Mechanical Engineers, Part L: Journal of Materials: Design and Applications*, doi: 10.1177/14644207211047376.

Pandian, A.K., Gautam, S.S. and Senthilvelan, S. (2022b), "Effect of layer orientation on the single tooth bending fatigue strength of polymer gears manufactured by selective laser sintering", *Proceedings of the Institution of Mechanical Engineers, Part L: Journal of Materials: Design and Applications*, doi: 10.1177/14644207221074902.

Petzold, S., Klett, J., Schauer, A. and Osswald, T.A. (2019), "Surface roughness of polyamide 12 parts manufactured using selective laser sintering", *Polymer Testing*, Vol. 80, p. 106094, doi: 10.1016/j.polymertesting.2019.106094.

Pilipovic, A., Valentan, B. and Šercer, M. (2016), "Influence of SLS processing parameters according to the new mathematical model on flexural properties", *Rapid Prototyping Journal*, Vol. 22 No. 2, doi: 10.1108/RPJ-08-2014-0092.

Raghunath, N. and Pandey, P.M. (2007), "Improving accuracy through shrinkage modelling by using Taguchi method in selective laser sintering", *International Journal of Machine Tools and Manufacture*, Vol. 47 No. 6, doi: 10.1016/j.ijmachtools.2006.07.001.

Schmid, M. (2018), "LS materials: polymer properties", *Laser Sintering with Plastics*, doi: 10.3139/9781569906842.004.

Schmid, M. and Wegener, K. (2016), "Additive manufacturing: polymers applicable for laser sintering (LS)", *Procedia Engineering*, Vol. 149, doi: 10.1016/j.proeng.2016.06.692.

Senthilkumaran, K., Pandey, P.M. and Rao, P.V.M. (2009), "Influence of building strategies on the accuracy of parts in selective laser sintering", *Materials & Design*, Vol. 30 No. 8, doi: 10.1016/j.matdes.2009.01.009.

Shackleford, A.S.D., Williams, R.J., Brown, R., Wingham, J.R. and Majewski, C. (2021), "Degradation of laser sintered polyamide 12 parts due to accelerated exposure to ultraviolet radiation", *Additive Manufacturing*, Vol. 46, p. 102132, doi: 10.1016/j.addma.2021.102132.

Shi, Y., Li, Z., Sun, H., Huang, S. and Zeng, F. (2004), "Effect of the properties of the polymer materials on the quality of selective laser sintering parts", *Proceedings of the Institution of Mechanical Engineers, Part L: Journal of Materials: Design and Applications*, doi: 10.1243/1464420041579454.

Singh, S., Sharma, V.S. and Sachdeva, A. (2012), "Optimization and analysis of shrinkage in selective laser sintered polyamide parts", *Materials and Manufacturing Processes*, Vol. 27 No. 6, doi: 10.1080/10426914.2011.593247.

Soe, S.P., Eyers, D.R. and Setchi, R. (2013), "Assessment of non-uniform shrinkage in the laser sintering of polymer materials", *The International Journal of Advanced Manufacturing Technology*, Vol. 68 Nos 1/4, doi: 10.1007/s00170-012-4712-0.

Spiegel, M.R. and Seymour Lipschutz, J.L. (2009), *Mathematical Handbook of Formulas and Tables*, McGraw Hill Professional, New York, NY.

Tunalioglu, M.S. and Agca, B.V. (2022), "Wear and service life of 3-D printed polymeric gears", *Polymers*, Vol. 14 No. 10, doi: 10.3390/polym14102064.

Verbelen, L., Dadbakhsh, S., Van Den Eynde, M., Kruth, J.P., Goderis, B. and Van Puyvelde, P. (2016), "Characterization of polyamide powders for determination of laser sintering processability", *European Polymer Journal*, Vol. 75, doi: 10.1016/j.eurpolymj.2015.12.014.

Vetterli, M., Schmid, M., Knapp, W. and Wegener, K. (2017), "New horizons in selective laser sintering surface roughness characterization", *Surface Topography: Metrology and Properties*, Vol. 5 No. 4, doi: 10.1088/2051-672x/aa88ee.

Wang, X. (1999), "Calibration of shrinkage and beam offset in SLS process", *Rapid Prototyping Journal*, Vol. 5 No. 3, doi: 10.1108/13552549910278955.

Watson, D. (2003), "Optimization of SLS process parameters using D-Optimality", *Solid Freeform Fabrication Proceedings*, pp. 348-362, doi: 10.26153/tsw/5570.

Wudy, K. and Drummer, D. (2019), "Aging effects of polyamide 12 in selective laser sintering: molecular weight distribution and thermal properties", *Additive Manufacturing*, Vol. 25, doi: 10.1016/j.addma.2018.11.007.

Yang, F., Jiang, T., Lalier, G., Bartolone, J. and Chen, X. (2020), "A process control and interlayer heating approach to reuse polyamide 12 powders and create parts with improved mechanical properties in selective laser sintering", *Journal of Manufacturing Processes*, Vol. 57, doi: 10.1016/j.jmapro.2020.07.051.

Yang, F., Zobeiry, N., Mamidala, R. and Chen, X. (2023), "A review of aging, degradation, and reusability of PA12 powders in selective laser sintering additive manufacturing", *Materials Today Communications*, Vol. 34, p. 105279, doi: 10.1016/j.mtcomm.2022.105279.

Yuan, M., Bourell, D. and Diller, T. (2011), "Thermal conductivity measurements of polyamide 12", *22nd Annual International Solid Freeform Fabrication Symposium – An Additive Manufacturing Conference, SFF 2011*.

Zhang, Y., Purssell, C., Mao, K. and Leigh, S. (2020), "A physical investigation of wear and thermal characteristics of 3D printed nylon spur gears", *Tribology International*, Vol. 141, p. 105953, doi: 10.1016/j.triboint.2019.105953.

Supplementary material

The supplementary data for this article can be found online.

Corresponding author

Flaviana Calignano can be contacted at: flaviana.calignano@polito.it